HHS Public Access

Author manuscript

Dev Biol. Author manuscript; available in PMC 2016 November 28.

Published in final edited form as:

Dev Biol. 2016 January 1; 409(1): 181–193. doi:10.1016/j.ydbio.2015.10.027.

The spatio-temporal domains of Frizzled6 action in planar polarity control of hair follicle orientation

Hao Chang[a,d], **Philip M. Smallwood**[a,d], **John Williams**[a,d], and **Jeremy Nathans**[a,b,c,d,*]

[a]Department of Molecular Biology and Genetics, Johns Hopkins University School of Medicine, Baltimore, MD 21205, United States

[b]Department of Neuroscience, Johns Hopkins University School of Medicine, Baltimore, MD 21205, United States

[c]Department of Ophthalmology, Johns Hopkins University School of Medicine, Baltimore, MD 21205, United States

[d]Howard Hughes Medical Institute, Johns Hopkins University School of Medicine, Baltimore, MD 21205, United States

Abstract

In mammals, hair follicles cover most of the body surface and exhibit precise and stereotyped orientations relative to the body axes. Follicle orientation is controlled by the planar cell polarity (PCP; or, more generally, tissue polarity) system, as determined by the follicle mis-orientation phenotypes observed in mice with PCP gene mutations. The present study uses conditional knockout alleles of the PCP genes *Frizzled6* (*Fz6*), *Vangl1*, and *Vangl2*, together with a series of *Cre* drivers to interrogate the spatio-temporal domains of PCP gene action in the developing mouse epidermis required for follicle orientation. *Fz6* is required starting between embryonic day (E)11.5 and E12.5. Eliminating *Fz6* in either the anterior or the posterior halves of the embryo or in either the feet or the torso leads to follicle mis-orientation phenotypes that are limited to the territories associated with *Fz6* loss, implying either that PCP signaling is required for communicating polarity information on a local but not a global scale, or that there are multiple independent sources of global polarity information. Eliminating *Fz6* in most hair follicle cells or in the inter-follicular epidermis at E15.5 suggests that PCP signaling in developing follicles is not required to maintain their orientation. The asymmetric arrangement of Merkel cells around the base of each guard hair follicle dependents on *Fz6* expression in the epidermis but not in differentiating Merkel cells. These experiments constrain current models of PCP signaling and the flow of polarity information in mammalian skin.

*Correspondence to: 805 PCTB, 725 North Wolfe Street, Johns Hopkins University School of Medicine, Baltimore, MD 21205, United States. Fax: +410 614 0827. jnathans@jhmi.edu (J. Nathans).

Author contributions

HC designed, conducted, and analyzed all of the experiments; JN designed and analyzed the experiments; HC and JN wrote the paper; JW constructed the *Vangl1*^{CKO} targeting plasmid; PMS constructed the *Fz6*^{CKO} targeting plasmid, and performed the ES cell targeting and initial characterization of the knockout lines.

Appendix A. Supplementary material

Supplementary data associated with this article can be found in the online version at http://dx.doi.Org/10.1016/j.ydbio.2015.10.027.

Keywords

Skin; Tissue polarity; Planar cell polarity; Mouse development; Merkel cell; *Fz6*; Vangl1; Vangl2

1. Introduction

In metazoan animals, the complex morphologies of cellular and multi-cellular structures appear to be genetically hard-wired as judged by their dramatic variation between species and their near constancy within species. One feature that characterizes many types of biological structures is polarity relative to local and/or global anatomic landmarks. A genetic system that controls polarity of this type has been extensively investigated in *Drosophila*, and is referred to as tissue polarity or planar cell polarity (PCP). PCP controls the chirality of ommatidia and the polarity of cuticular hairs and bristles, and it is mediated by a small number of genes that code for integral membrane proteins and membrane-associated cytoplasmic proteins (Adler, 2002; Jenny, 2010; Goodrich and Strutt, 2011). In epithelia, the asymmetric localization of PCP proteins marks each cell with an orientation vector within the plane of the epithelium.

In vertebrates, homologues have been identified for each of the *Drosophila* PCP genes. In mice, mutation of these genes demonstrates their central role in controlling polarity in a wide variety of contexts, including neural tube closure (Wang et al., 2006b; Torban et al., 2008; Curtin et al., 2003), axon guidance (Wang et al., 2002; Lyuksyutova et al., 2003; Tissir et al., 2005; Zhou et al., 2008; Hua et al., 2013, 2014b), and the orientations of motile cilia (Tissir et al., 2010; Vladar et al. 2012; Boutin et al., 2014; Ohata et al., 2014; Shi et al., 2014), inner ear sensory hair cells (Montcouquiol et al., 2003; Wang et al., 2005, 2006b; Jones et al., 2014), hair follicles (Guo et al., 2004; Wang et al., 2006a; Devenport and Fuchs, 2008; Ravni et al., 2009), and lingual papillae (Hua et al., 2014a).

Mammalian hair follicles form by invagination of surface epithelial cells into the dermis, and they generally exhibit an orientation that is oblique to the plane of the epithelium. Mutations in the PCP genes *Fz6*, *Celsr1*, and *Vangl2* produce hair follicle orientation phenotypes. In $Fz6^{-/-}$ fetuses and neonates, the orientations of hair follicles in back skin appear to be nearly randomized, implying that PCP signaling is required for the initial orientations relative to the body axes (Wang et al., 2006a, 2010). As development proceeds, a Fz6-independent process causes follicles to progressively reorient within the dermis in a manner that minimizes angular differences between neighboring follicles. The result is a series of enlarging patterns, including whorls and cruciforms.

A set of central and unanswered questions in the PCP field relates to the source and timing of polarity information and the manner in which that information propagates across tissues and between distinct cellular structures. In the vertebrate epidermis, the identities of the anterior/posterior polarity signals on the trunk and the proximal/distal polarity signals on the limbs are currently unknown. With spatially and temporally defined manipulations of gene activity in mice it may be possible to constrain models concerning the nature of these signals and their relationship to PCP signaling. With this idea in mind, we have used anatomically localized and cell-type specific Cre-mediated recombination to create spatial and temporal

patterns of Fz6 activity to determine when polarity information is acquired, and whether this information exhibits an obligatory flow from one part of the embryo to another, and whether Fz6 is required in developing follicles to maintain their orientation and in Merkel cells to produce an asymmetric cell cluster. The results imply that, in the mouse epidermis, Fz6-dependent polarity signaling begins at embryonic day (E)12 and that there are multiple sources of global polarity information.

2. Results

2.1. Timing of Fz6 expression for hair follicle orientation

On the head and back of wild type (*WT*) mice, hair follicles point with high precision from anterior to posterior, and, as noted in the Introduction, this global polarity is largely absent in fetal and early postnatal $Fz6^{-/-}$ mice. In a first set of experiments, we investigated the critical time window for Fz6-dependent signaling, by eliminating or activating *Fz6* expression with an epidermal-specific *K14-Cre* transgene (Dassule et al., 2000) that initiates *Cre* expression at nearly the same time as the endogenous *Fz6* gene. In the developing epidermis on the back, Fz6 is initially detected at E12.5 and it continues to be expressed throughout fetal life (Fig. 1A and S1). One day later, at E13.5, placodes appear at the locations of future guard hair follicles (Ahn, 2015). Expression of the *K14-Cre* transgene begins between E11.5 and E12.5, as determined by crossing it to *Hprt-LSL-tdT*, a highly recombinogenic reporter that expresses a nuclear-localized 3HA-tagged tdTomato (Fig. 1B; LSL represents loxP-stop-loxP; Wu et al., 2014). [See Table 1 for a summary of the temporal patterns of *Cre* expression in the mouse lines used in this study.]

Using *K14-Cre* to inactivate a conditional *Fz6* knockout allele (Fig. S2) in $Fz6^{CKO/-}$;*K14-Cre* mice, we observed the transient appearance of Fz6 at E12.5, followed by its disappearance one day later (Fig. 1C). The phenotypic consequences of eliminating *Fz6* from E13.5 onward is a follicle mis-orientation phenotype on the back and head at postnatal day (P)3 that is significantly milder than the $Fz6^{-/-}$ phenotype (quantified in Fig. 1D), suggesting that transient expression of *Fz6* at E12.5 allowed the developing epidermis to partially acquire global polarity. We note that the possible perdurance of Fz6, at levels below the limit of detection, could extend the window of Fz6 action beyond E12.5. The same *K14-Cre* transgene was used to activate *Fz6* expression from a *Rosa(R)26-LSL-Fz6* knock-in allele on a $Fz6^{-/-}$ background. In earlier work, we observed that Cre-mediated recombination of the *R26-LSL-Fz6* locus in the parental germline led to ubiquitous expression of *Fz6* in the skin at approximately the same level as the endogenous *Fz6* gene and to a full rescue the $Fz6^{-/-}$ phenotype (Hua et al., 2014a). Fig. 1D shows that $Fz6^{-/-}$;*R26-LSL-Fz6;K14-Cre* mice have a *WT* hair orientation phenotype. These data imply that Fz6-mediated polarity signaling in the epidermis of the back and head begins between E11.5 and E12.5.

2.2. Effect of anterior or posterior expression of Fz6 on hair follicle orientation

We next sought to test the hypothesis that global polarity information originates from a single source in either the anterior or the posterior of the embryo and propagates across the surface epithelium in a Fz6-dependent manner. The experimental strategy involved

eliminating *Fz6* exclusively in either the anterior or posterior halves of the embryo. For selective deletion of *Fz6* in posterior territories we used a *Caudal2 (Cdx2)-Cre* transgene (Hinoi et al., 2007), which is expressed in all or nearly all embryonic tissues, including the ectoderm, posterior to the insertion of the umbilical vessels. *Cdx2-Cre* expression begins before E11.5, a time prior to the initiation of *Fz6* expression (Fig. 2A and S3; Table 1). We will refer to $Fz6^{CKO/-}$;*Cdx2-Cre* embryos as "posterior *Fz6* KO".

At present, there are no *Cre* lines that uniformly recombine anterior structures in a spatial pattern that is complementary to the pattern of *Cdx2-Cre* expression. Therefore, to eliminate *Fz6* in the anterior of the embryo, we used an indirect strategy in which *Cdx2-Cre* -mediated recombination activated *Fz6* expression from the *R26-LSL-Fz6* locus in the posterior of $Fz6^{-/-}$ embryos. As this combination of ubiquitous loss of endogenous *Fz6* and posterior-specific expression of ectopic *Fz6* is equivalent to an anterior-specific elimination of *Fz6*, we will refer to it as "anterior *Fz6 KO*".

In preliminary experiments, we compared the levels of Fz6 accumulation in cross-sections of skin at E14.5 in anterior and posterior locations (the neck and lower back, respectively) in *WT,* $Fz6^{CKO/-}$;*Cdx2-Cre* ("posterior *Fz6* KO"), $Fz6^{-/-}$;*R26-LSL-Fz6;Cdx2-Cre* ("anterior *Fz6* KO"), and $Fz6^{-/-}$ embryos (Fig. 2B). As expected, Fz6 is present in *WT* epidermis and absent in $Fz6^{-/-}$ epidermis. In the "posterior *Fz6* KO" embryo, Fz6 is present in the anterior but not the posterior epidermis. In the "anterior *Fz6* KO", Fz6 is present in both the epidermis and dermis in the posterior of the embryo, consistent with expression of the *R26* locus in most if not all cell types, but Fz6 is absent in the anterior of the embryo.

Hair follicle orientations were quantified in anterior (head) and posterior (lower back) regions in flat mounted skins from *WT*, "posterior *Fz6* KO", "anterior *Fz6* KO", and $Fz6^{-/-}$ mice at P3 (Fig. 2C). At this age, follicles in $Fz6^{-/-}$ mice exhibit a broad distribution of orientations with a subtle anterior-to-posterior bias. In contrast, *WT* mice show a narrow distribution centered on the anterior-to-posterior vector. "Posterior *Fz6* KO" and "anterior *Fz6* KO" mice show broad distributions of follicle orientations in the territories lacking *Fz6* expression and normal anterior-to-posterior follicle orientations in those regions where *Fz6* is expressed.

To visualize and quantify follicle orientations at the earliest stage of development (and prior to the accumulation of melanin within the follicle), back skins from the same four genotypes were examined at E17.5 in the presence of a *Keratin(K)17-GFP* transgene, which is expressed specifically in hair follicles (Bianchi et al., 2005). For this experiment, the *Hprt-LSL-tdT* reporter was also present to simultaneously demarcate the zone of *Cdx2-Cre* activity. At E17.5, the developing guard hair follicles are the only follicles that have elongated sufficiently to permit a determination of orientation. As seen in Fig. 3, the boundary between the anterior zone with undetectable Cre-mediated recombination and the posterior zone with high Cre-mediated recombination extends over several millimeters along the anterior-posterior axis. In the $Fz6^{-/-}$ back skin (bottom panel in Fig. 3), the distribution of follicle orientations shows the same subtle posterior bias as at P3, implying that loss of *Fz6* does not lead to a complete randomization of the initial follicle orientations. In "posterior *Fz6* KO" back skin, the territories of follicle mis-orientation and *Cdx2-Cre* are

closely matched (second panel in Fig. 3). Interestingly, in the "anterior *Fz6* KO" back skin (third panel in Fig. 3), follicles anterior to and within several millimeters of the zone of Cre-recombination are largely oriented in an anterior-to-posterior direction, despite the inference from the *Hprt-LSL-tdT* reporter that they are predominantly $Fz6^{-/-}$. These data imply that polarity information can spread over a limited distance through $Fz6^{-/-}$ tissue or through tissue that contains a mixture of Fz6-expressing and Fz6-null epithelial cells.

The analysis of hair follicle orientations in the back skin of "anterior *Fz6* KO" and "posterior *Fz6* KO" fetuses and postnatal mice eliminates one model in which global polarity information originates from a unique source in either the anterior or the posterior poles of the embryo and then propagates across the surface epithelium in a Fz6-dependent manner. Such a model predicts that a zone of $Fz6^{-/-}$tissue adjacent to the source of polarity information would block its propagation to more distal territories. However, these experiments do not eliminate models in which polarity information originates from both anterior and posterior poles or propagates across the embryo by a mechanism that is independent of Fz6.

2.3. Effect of limb-specific expression or knockout of Fz6 on hair follicle orientation

On the dorsal surface of the feet of *WT* mice, hair follicles at all stages of development point from the proximal limb distally toward the digits and the palmar surface, and no follicles exhibit a distal-to-proximal orientation. In contrast, in $Fz6^{-/-}$ mice, many early postnatal follicles on the dorsal surface of the feet exhibit a distal-to-proximal orientation, and during the first postnatal week these follicles reorganize to produce a single whorl on each hindfoot and a milder whorl-like pattern on each front foot (Guo et al., 2004; Wang et al., 2006a, 2010). To investigate the possible flow of polarity information from torso to limb, we employed an experimental strategy analogous to that described above for the anterior-posterior axis, but using instead an *Emx1-Cre* knock-in allele that is expressed specifically in the limb bud ectoderm prior to E11.5 (Fig. 4A and S3; Table 1; Gorski et al., 2002). To eliminate *Fz6* in the distal limb ectoderm, we generated $Fz6^{CKO/-}$*;Emx1-Cre* mice that we will refer to as "foot-specific *Fz6* KO". To eliminate *Fz6* everywhere except in the distal limb ectoderm, we generated $Fz6^{-/-}$*;R26-LSL-Fz6;Emx1-Cre* mice, which we will refer to as "torso-specific *Fz6* KO".

Hair follicle orientations were quantified in flat mounts of foot skin at P4 and back skin at P3 from *WT,* $Fz6^{CKO/-}$*;Emx1-Cre* ("foot-specific *Fz6* KO"), $FZ6^{-/-}$*;R26-LSL-Fz6;Emx1-Cre* ("torso-specific *Fz6* KO"), and $Fz6^{-/-}$ mice (Fig. 4B). At P4, *WT* foot skins show a distribution of orientations from −90 to +90 degrees, reflecting the range of follicle orientations that point from the dorsal surface of the foot toward the palmar surface, especially around the periphery of the foot. In contrast, P4 $Fz6^{-/-}$ foot skins have many follicles with distal-to-proximal orientations (90–180 degrees and from −180 to −90 degrees). In "torso-specific *Fz6* KO" mice at P3, as well as at later ages (data not shown), follicle orientations on the feet are indistinguishable from *WT*. Similarly, in "foot-specific *Fz6* KO" mice at P3, as well as at later stages (data not shown), follicle orientations on the feet are indistinguishable from the orientations observed on $Fz6^{-/-}$ feet. These data imply

that epidermal polarity on the feet is dependent on the local activity of Fz6 and is independent of Fz6 activity in the torso.

2.4. Effects of hair follicle-specific versus epidermis-specific Fz6 expression and knockout

If polarity information for determining hair follicle orientation is propagated across the epidermis by PCP signaling, then disrupting PCP signaling specifically in the inter-follicular epidermis should block the flow of information and cause follicle mis-orientation. Additionally, depending on the manner in which follicles receive and process polarity information, disruption of PCP signaling specifically within follicles might also lead to a follicle mis-orientation phenotype. These predictions are compatible with the timing of *Fz6* expression that we observe in the epidermis: as noted above in the context of Fig. 1, *Fz6* expression begins at E11.5-E12.5, and by E13.5, when guard hair placodes first appear, it is expressed uniformly in the epidermis on the back.

At present, there is no mouse line that expresses *Cre* exclusively in all inter-follicular epidermal cells or exclusively in all hair follicle epithelial cells. However, *Shh* is expressed in a subset of epithelial cells within hair follicles as early as E14.5 (Bitgood and McMahon, 1995), and *Shh-Cre* (a *Cre* knock-in at the *Shh* locus; Harfe et al., 2004) recombines the *Hprt-LSL-tdT* reporter in > 50% of developing guard hair follicle epithelial cells by E15.5 (Fig. 5A, right panels). *Shh-Cre*-induced expression of the tdTomato reporter was not observed in hair follicles prior to E15.5 or in the inter-follicular epidermis at any time (Table 1). By E15.5, *Fz6* expression is readily detected in both developing guard hair follicles and inter-follicular epidermis, and developing guard hair follicles are already correctly oriented along the anterior-posterior axis (Fig. 5A, left).

To investigate the role of *Fz6* in maintaining follicle orientation after E15.5, we designed an experimental strategy analogous to that described above for the anterior-posterior axis and the feet. To eliminate *Fz6* in a subset of follicle epithelial cells starting at E15.5, we generated $Fz6^{CKO/-}$;*Shh-Cre* mice, which we will refer to as "follicular *Fz6* KO", and to eliminate *Fz6* in the inter-follicular epithelium at all times, we generated $Fz6^{-/-}$;*R26-LSL-Fz6;Shh-Cre* mice, which we will refer to as "inter-follicular *Fz6* KO". In preliminary experiments, we compared the levels of Fz6 accumulation in cross-sections of E15.5 back skin in *WT*, $Fz6^{CKO/-}$;*Shh-Cre* ("follicular *Fz6* KO"), $Fz6^{-/-}$;*R26-LSL-Fz6;Shh-Cre* ("inter-follicular *Fz6* KO"), and $Fz6^{-/-}$ embryos (Fig. 5B). As expected, Fz6 is observed throughout the epidermis and in developing guard hair follicles in *WT* embryos, and it is absent in $Fz6^{-/-}$ embryos. In the "follicular *Fz6* KO", Fz6 is detected at higher levels in the inter-follicular epidermis than in follicles. In the "inter-follicular *Fz6* KO", Fz6 is detected only in hair follicles.

Hair follicle orientations were quantified in flat mounted skins from P3 mice of the same four genotypes. "Inter-follicular *Fz6* KO" mice exhibit a follicle mis-orientation phenotype equal in severity to that of $Fz6^{-/-}$ mice, whereas, "follicular *Fz6* KO" mice exhibit a distribution of follicle orientations similar to that of *WT* controls. These data are consistent with the observations of Devenport and Fuchs (2008) with *WT*:$Vangl2^{Lp/Lp}$ chimeras showing that when a WT follicle is flanked by $Vangl2^{Lp/Lp}$ epidermis, the follicle exhibits the vertical $Vangl2^{Lp/Lp}$ phenotype. In interpreting this experiment, we note that *Shh-Cre*

does not act until E14.5-E15.5, 1–2 days after guard hair placodes appear, at which time developing guard hair follicles are already oriented along the anterior-to-posterior axis (Fig. 5A and B). Thus, this experiment is relevant to the maintenance but not to the initiation of follicle orientation. With the additional caveat that *Shh-Cre* does not eliminate *Fz6* expression in all follicle cells in the "follicle *Fz6* KO" or activate *Fz6* expression in all follicle cells in the "inter-follicular *Fz6* KO", the data suggest that the maintenance of the anterior-to-posterior orientation during follicle elongation does not require *Fz6* expression in more than a minority of follicle cells after E15.5. The data are also consistent with a model in which PCP signaling prior to E14.5-E15.5 sets the orientation of follicle growth.

2.5. Effects of Merkel cell-specific Fz6 expression and knockout

Hair follicles are associated with a variety of non-follicle structures, each of which normally exhibits a polarity that matches the polarity of its associated follicle. These structures include sebaceous glands, arrector pili muscles, sensory nerve endings, and Merkel cell clusters (Ross and Pawlina, 2011). In $Fz6^{-/-}$ mice, sebaceous glands, arrector pili muscles, and sensory nerve endings reorient to track the aberrant orientation of their associated follicles (Chang and Nathans, 2013). In contrast, Merkel cell clusters lose their polarity in the absence of *Fz6*. The ~30 Merkel cells at the base of each guard hair follicle are arranged in a semi-circle with an anterior opening in *WT* skin, but they form a closed circle in $Fz6^{-/-}$ skin (Chang and Nathans, 2013). We note that Merkel cells are epidermal derivatives, and therefore it is not surprising that they are directly influenced by PCP signals.

To investigate the flow of polarity information to Merkel cells, we utilized a *Math1(Atoh1)-Cre* knock-in line that expresses *Cre* in Merkel cells starting at E15.5 when Merkel cells begin to differentiate (Fig. 6A; Yang et al., 2010). Using the *Math1-Cre* line, we designed an experimental strategy analogous to that described above for hair follicles and inter-follicular epidermis (Fig. 6B). To eliminate *Fz6* in Merkel cells, we generated $Fz6^{CKO/-}$*;Math1-Cre* mice, which we will refer to as "Merkel cell *Fz6* KO", and to eliminate *Fz6* in all epidermal derivatives other than Merkel cells, we generated $Fz6^{-/-}$*;R26-LSL-Fz6;Math1-Cre* mice, which we will refer to as "non-Merkel cell *Fz6* KO".

In flat mounts of skin at P1, a time when Merkel cell clusters are fully developed, the arrangement of Merkel cells in "Merkel cell *Fz6* KO" mice was indistinguishable from *WT* mice, and the arrangement of Merkel cells in "non-Merkel cell *Fz6* KO" mice was indistinguishable from $Fz6^{-/-}$ mice (Fig. 6C). The data were quantified by measuring the size of the largest angular opening in each Merkel cell cluster and the fraction of Merkel cells that reside anterior to the center of each cluster (Fig. 6C; Chang and Nathans, 2013). In interpreting these experiments we note the possibility that the *WT* polarity of Merkel cell clusters in "Merkel cell *Fz6* KO" mice might reflect the perdurance of Fz6 proteins that had accumulated prior to *Math1-Cre*-mediated *Fz6* deletion between E14.5-E15.5. While keeping this caveat in mind, this experiment suggests is that the anterior-facing semi-circular arrangement of Merkel cells does not require *Fz6* expression in Merkel cells during the time when the semi-circle is being formed.

2.6. Roles of Vangl1 and Vangl2 in hair follicle orientation

To test the generality of the spatial and temporal effects of *Fz6* deletion, we asked whether deleting *Vangl1* and *Vangl2* - the only two mammalian orthologues of the *Drosophila* core PCP gene *Vang* - using *K14-Cre* or *Cdx2-Cre* would produce the same phenotypes as observed with deletion of *Fz6*. In previous work, we and others observed a loss of follicle polarity in fetuses homozygous for the *semi-dominant Vangl2 Looptail (Lp*) allele (Devenport and Fuchs, 2008; Wang et al., 2010). As $Vangl2^{Lp/Lp}$ mice die at birth, this follicle phenotype could only be examined during prenatal life. Curiously, prenatal $Vangl2^{Lp/Lp}$ follicles are oriented perpendicular to the plane of the epithelium. This phenotype is distinct from the $Fz6^{-/-}$ phenotype in which follicles are mis-oriented but retain their oblique angle to the epithelial plane.

Vangl1 and/or *Vangl2* recessive loss-of-function mutations have been studied previously in the early embryo in the context of left-right asymmetry, in neural tube closure, and in inner ear development (Torban et al., 2008; Song et al., 2010; Copley et al., 2013; Pryor et al., 2014), but they have not been studied in the skin. To eliminate *Vangl1* and/or *Vangl2* in various allelic combinations in the epidermis we constructed a $Vangl1^{CKO}$ allele (Fig. S4) and combined it with a $Vangl2^{CKO}$ allele (Yin et al., 2012) and the *K14-Cre* transgene to generate mice in which different numbers of *Vangl1* and *Vangl2* alleles were deleted.

Eliminating one allele each of *Vangl1* and *Vangl2* in the epidermis at E12.5 with *K14-Cre* ($Vangl1^{CKO/+};Vangl2^{CKO/+};K14\text{-}Cre$) or ubiquitously ($Vangl1^{CKO/-};Vangl2^{CKO/-}$, without *Cre*) had no effect on follicle orientations. However, eliminating all four Vangl alleles in the epidermis ($Vangl1^{CKO/-};Vangl2^{CKO/-};K14\text{-}Cre$) led to vertically oriented hair follicles in prenatal skin at E16.5 that closely resembled the phenotype observed with $Vangl2^{Lp/Lp}$ (Fig. 7A). By P3, follicles in $Vang/1^{CKO/-};Vang/2^{CKO/-};K14\text{-}Cre$ mice had acquired an oblique angle relative to the epithelial surface and exhibited largely randomized orientations on the back and partially randomized orientations on the head (Fig. 7B). A comparison of follicle angles at P3 between $Fz6^{CKO/-};K14\text{-}Cre$ mice (Fig. 1D, second from left) and $Vangl1^{CKO/-};Vangl2^{CKO/-};K14\text{-}Cre$ mice (Fig. 7B, far right) revealed a more severe phenotype in $Vang/1^{CKO/-};Vangl2^{CKO/-};K14\text{-}Cre$ mice. Together with the distinctive phenotype of vertically oriented follicles, these observations suggest that a more extensive loss of PCP signaling is produced by the combined loss of *Vangl1* and *Vangl2* than by loss of *Fz6*.

At P3, $Vangl1^{CKO/-};Vangl2^{CKO/-}$ mice (loss of one allele each of *Vangl* and *Vangl2*) and $Vangl1^{CKO/-};Vangl2^{CKOI+};K14\text{-}Cre$ mice (loss of two alleles of Vang1 and one allele *Vangl2*) exhibit head and back follicle orientations that closely resemble those of the *WT* control, whereas $Vangl1^{CKO/+};Vangl2^{CKO/-};K14\text{-}Cre$ mice (loss of one alleles of *Vangl* and two alleles of *Vangl2*) exhibit a phenotype intermediate between $Vangl1^{CKO/-};Vangl2^{CKO/-};K14\text{-}Cre$ mice (loss of all four alleles) and *WT* mice (Fig. 7B). From these data we conclude that *Vangl2* plays a larger role than *Vangl1* in follicle orientation.

When *Vangl1* and *Vangl2* were deleted in the posterior of the body with *Cdx2-Cre* ($Vangl1^{CKO/-}, Vangl2^{CKO/-}, Cdx2\text{-}Cre$), > 95% of mice died shortly after birth, with most

showing a caudal neural tube defect, tail truncation, and retarded growth of the hind limbs (Fig. 7C and S5). The single *Vangl1*$^{CKO/-}$;*Vangl2*$^{CKO/-}$;*Cdx2-Cre* mouse that did not have an open neural tube was analyzed at P3 and exhibited hair follicle orientations that were largely randomized on the lower back but not on the head (Fig. 7C, right panels), consistent with the pattern observed in *Fz6*$^{CKO/-}$;*Cdx2-Cre* mice. Additionally, *Vangl1*$^{CKO/-}$;*Vangl2*$^{CKO/-}$;*K14-Cre* mice show the same circular arrangement of Merkel cells as observed in *Fz6*$^{-/-}$ mice, *Vangl1*$^{CKO/-}$;*Vangl2*$^{CKO/-}$;*Shh-Cre* show normal hair follicle orientations as observed in *Fz6*$^{CKO/-}$;*Shh-Cre* mice, and *Vangl1*$^{CKO/-}$;*Vangl2*$^{CKO/-}$;Math1-Cre mice show a normal arrangement of Merkel cells as observed in *Fz6*$^{CKO/-}$;Math1-Cre mice (data not shown). These observations support the view that *Fz6* and *Vangl1/Vangl2* work together to mediate PCP signaling in the epithelium.

3. Discussion

The body of work presented here represents the first systematic study of the spatiotemporal characteristics of mammalian PCP signaling in epithelial development. Utilizing a series of *Cre* driver lines with well-defined spatiotemporal patterns of expression, we have conditionally deleted *Fz6* or *Vangl1* and *Vangl2* in different anatomic patterns and at different times in the mouse epidermis and in various epidermal derivatives. To compare the polarity phenotypes associated with *Fz6* loss in anatomically reciprocal pairs of territories or cell types, we devised a strategy in which the phenotype produced by *Fz6* deletion using a particular *Cre* driver is compared to the phenotype produced by ectopic *Fz6* activation using the same *Cre* driver in the absence of endogenous *Fz6*. As described below, the results of these experiments constrain potential models of PCP signaling in the mammalian epidermis.

3.1. Timing of Fz6 expression and action

In the absence of *Fz6*, the initial follicle polarities on the head are largely randomized and those on the back are almost completely randomized. One model consistent with this phenotype posits that Fz6 acts as part of a system to propagate polarity information across the surface epithelium from source(s) at the extreme anterior and/or posterior of the embryo. Alternatively, one can envision models in which Fz6 only communicates polarity information locally, in which case other polarity systems would need to be invoked to set-up polarity on the scale of the entire embryo. In *Drosophila*, experiments with marked clones clearly demonstrate a role for PCP signaling in the local spread of polarity information, but they are also consistent with a role for PCP genes in setting up polarity on a larger scale (Adler, 2002; Strutt and Strutt, 2005; Goodrich and Strutt, 2011; Struhl et al., 2012).

In mice, the earliest developing hair follicles do not begin to appear until E13.5, when the embryo is ~12 mm in length (Kaufman, 1992). It would be remarkable if global polarity information could propagate across an embryo of this size. Instead, it seems more reasonable to suppose that anterior–posterior polarity information is generated when the embryo is far smaller and that this information is preserved and made available to the epidermis at later times. Following this line of reasoning, the experiments described here to determine the time window during which Fz6 acts can potentially constrain models of local vs. global roles for Fz6.

It has long been known that *Fz6* is expressed in the epidermis and in hair follicles during late fetal and adult life (Guo et al., 2004). Here we show that Fz6 is not detectable in the epidermis by immunostaining prior to E12.5. We note, however, that physical analyses of gene expression - by immunostaining, in situ hybridization, detection of knock-in reporters, etc. - cannot be considered definitive methods for assessing the time and place of gene action because extremely low levels of gene expression can potentially provide biological function. Indeed, earlier experiments with $Fz3^{-/-};Fz6^{-/-}$ embryos demonstrated a redundant role for Fz3 and *Fz6* in neural tube closure, even though *Fz6* gene expression was undetectable, as determined by X-gal staining with a *lacZ* reporter knock-in, at the time of neural tube closure (~E8.5; Wang et al., 2006b).

Using *K14-Cre*, we have studied embryos with timed deletion or activation of Fz6. These experiments show that the critical time window for Fz6 function in hair follicle orientation begins at E11.5-E12.5 and continues at least through E13.5. Epidermal deletion of *Vangl1* and *Vangl2* at E11.5-E12.5 leads to a similar hair orientation phenotype. These results imply that Fz6-dependent PCP signaling begins early in epidermal development when the embryo is ~ 6 mm in length, 1–2 days prior to the appearance of hair follicle placodes. Compared to the most fundamental embryologic events (e.g. gastrulation), E11.5-E12.5 is relatively late, and the data therefore seem most compatible with a model in which Fz6 acts within the epidermis to locally interpret pre-existing polarity information.

3.2. Anatomic domains of Fz6 action: local influence within a global pattern

Direct tests of a role for Fz6 in propagating polarity information from a discrete source are described here in the contexts of anterior-posterior polarity on the head and torso and proximal-distal polarity in the limbs. In both contexts, early acting (i.e., before E11.5) and anatomically-localized *Cre* drivers allowed *Fz6* gene activity to be selectively eliminated in complementary regions of the epithelium: anterior vs. posterior halves of the embryo, and limb vs. torso. The resulting phenotypes show that (1) hair follicles require local expression of *Fz6* to attain their correct initial orientations, and (2) they are unaffected by the absence of *Fz6* in adjacent territories. Moreover, the intermediate PCP phenotype produced by transient expression of *Fz6* prior to K74-Cre-mediated inactivation in $Fz6^{CKO/-};K14\text{-}Cre$ embryos showed no anterior-posterior variation in severity, as might have been predicted if Fz6 effects the propagation of polarity information from one end of the embryo to the other over the course of hours to days. Taken together, the data are most compatible with a model in which Fz6 - and, by inference, PCP signaling generally - acts to locally communicate, stabilize, and/or transduce polarity information, but it does not constitute the sole means for transmitting that information over long distances.

We note that the preceding conclusions refer to the initial orientations of hair follicles. Later, during the first 8–10 days of postnatal life, a Fz6-independent system of communication generates and refines patterns of follicle orientation that eventually encompass many thousands of follicles (Wang et al., 2006a, 2010). This later refinement process can be accurately modeled as a local interaction between follicles that favors a convergence of orientations among neighbors (Wang et al., 2006a). Although its molecular and cellular mechanisms are unknown, this refinement process exemplifies one way in which polarity

information evolves and propagates across a vector field. A conceptually analogous system underlies the cooperative alignment of magnetic dipole moments among individual atoms in ferromagnetic materials (Feynman et al., 1963).

3.3. Acquisition of polarity information by Merkel cells and hair follicles

A major distinction between PCP in the mammalian epidermis and the *Drosophila* wing is that the former involves the polarized architectures of multicellular structures (hair follicles and Merkel cell clusters) whereas the latter only affects the orientations of subcellular structures (the actin-rich bundles that form the core of the wing hairs produced by each epithelial cell; Adler, 2002; Goodrich and Strutt, 2011). How individual cells within a multicellular structure acquire and differentially interpret polarity information to generate a coordinated spatial response is, at present, unknown.

The experiments described here with follicle-specific expression or deletion of *Fz6* and Merkel cell-specific expression or deletion of *Fz6* are consistent with a model in which polarity information from the surrounding epidermis influences the orientations of multi-cellular epithelium-derived structures. In the future it would be interesting to examine the way in which cell movements, cell proliferation and/or cell death shape architectural asymmetry in hair follicles and Merkel cell clusters. With the development of two-photon microscopic techniques for chronic imaging of identified cells in mammalian hair follicles (Mesa et al., 2015), it might be possible to investigate this question by monitoring epithelial cell behaviors longitudinally in ex vivo preparations of mouse embryos that are either *WT* or mutant for various PCP genes.

4. Materials and methods

4.1. Mouse lines

The $Fz6^{CKO}$ and $Vangl1^{CKO}$ alleles were generated by homologous recombination in mouse embryonic stem (ES) cells using standard techniques. In brief, targeting constructs (Fig. S2 and S4) were electroporated into R1 mouse ES cells; colonies were grown in medium containing G418 and ganclovir, and were screened by Southern blot hybridization; positive clones with a normal karyotype were injected into C57BL/6 blastocysts to generate chimeric founders; and germline transmission was confirmed by Southern blot hybridization and PCR.

The following mouse alleles were also used: $Fz6^{-}$ (Guo et al., 2004), *R26-LSL-FZ6* (Hua et al., 2014a,b), *Hprt-LSL-tdT* (Wu et al., 2014), K17-GFP (Bianchi et al., 2005), *Sox2-Cre* (Hayashi et al., 2002), *K14-Cre* (Dassule et al., 2000; JAX 004782), *Cdx2-Cre* (Hinoi et al., 2007; JAX 009350), *Emx1-Cre* (Gorski et al., 2002; JAX 005628), *Shh-Cre* (Harfe et al., 2004; JAX 005622), *Math1(Atoh1)-Cre* (Yang et al., 2010; a kind gift of Dr. Lin Gan, University of Rochester), $Vangl2^{CKO}$ (Copley et al., 2013), and $Vangl2^{-}$ (Smallwood, Williams, and Nathans, unpublished). Mice were handled and housed according to the approved Institutional Animal Care and Use Committee (IACUC) protocol M013M469 of the Johns Hopkins Medical Institutions.

4.2. Immunostaining

For immunostaining of sagittal sections, embryos were embedded in OCT, fresh frozen, cryosectioned (14 μm) and fixed for 10 min in 4% formaldehyde in PBS. Sections were washed with PBST (0.1% Triton in PBS) for 10 min and blocked for 1 h with 5% normal donkey or goat serum in PBST. Primary antibodies were incubated for 2 h at room temperature or overnight at 4 degree. The following primary antibodies were used: goat anti-Fz6 (AF1526; R and D Systems; 1:400), rat anti-E-cadherin (ab11512-100; Abcam; 1:400) and rat anti-Cytokeratin8 (TROMA-I-c; Developmental Studies Hybridoma Bank; 1:500). Secondary antibodies in PBST were incubated for one hour at RT. Secondary antibodies were Alexa Fluor 488-, 594-, or 647-conjugated donkey anti-goat, donkey anti-rat, or goat anti-rat IgG antibodies (Invitrogen; Grand Island, NY). Finally, sections were washed three times in PBST and mounted on slides with Fluoromount-G (Southern Biotech; Birmingham, AL).

For visualizing tdTomato's native fluorescent signal, embryos were fixed for 30 min with 4% formaldehyde in PBS and treated with progressively increasing sucrose concentrations (10%, 20%, 30% in PBS) before cryosectioning. Immunostained samples were imaged using a Zeiss LSM700 confocal microscope with Zen software.

4.3. Skin whole mounts

The procedures for preparation and processing of skin whole mounts for Merkel cell immunostaining and for imaging of hair follicles based on melanin content are described in Chang and Nathans (2013) and Chang et al. (2014). P3 whole mount skins processed for melanin were imaged using a Zeiss Stemi V11 microscope with a color Axiocam CCD in combination with Openlab software. Follicle orientations relative to the anterior-posterior (A–P) axis were quantified for three mice per genotype, except for the *Vangl1*$^{CKO/-}$*;Vangl2*$^{CKO/-}$*;Cdx2-Cre* genotype shown in Fig. 7C, for which only a single postnatal mouse survived. For each skin image, orientations relative to the A–P axis were determined for a set of 81 follicles closest to the grid points on a 9 × 9 grid encompassing 3.2 × 2.5 mm^2.

4.4. Skeleton staining and X-gal staining

The procedures for X-gal staining and whole-mount alcian blue and alizarin red staining of cartilage and bone from embryos are described by Nagy et al. (2003).

Supplementary Material

Refer to Web version on PubMed Central for supplementary material.

Acknowledgments

Supported by the Howard Hughes Medical Institute. The authors thank Dr. Amir Rattner for helpful comments on the manuscript.

References

Adler PN. Planar signaling and morphogenesis in Drosophila. Dev. Cell. 2002; 2:525–535. [PubMed: 12015961]

Ahn Y. Signaling in tooth, hair, and mammary placodes. Curr. Top. Dev. Biol. 2015; 111:421–459. [PubMed: 25662268]

Bianchi N, Depianto D, McGowan K, Gu C, Coulombe P. Exploiting the keratin 17 gene promoter to visualize live cells in epithelial appendages of mice. Mol. Cell. Biol. 2005; 25:7249–7259. [PubMed: 16055733]

Bitgood MJ, McMahon AP. Hedgehog and Bmp genes are coexpressed at many diverse sites of cell-cell interaction in the mouse embryo. Dev. Biol. 1995; 172:126–138. [PubMed: 7589793]

Boutin C, Labedan P, Dimidschstein J, Richard E, Cremer H, Andre P, Yang Y, Montcouquiol M, Goffinet AM, Tissir E. A dual role for planar cell polarity genes in ciliated cells. Proc. Natl. Acad. Sci. USA. 2014; 111:E3129–E3138. [PubMed: 25024228]

Chang H, Nathans J. Responses of hair follicle-associated structures to loss of planar cell polarity signaling. Proc. Natl. Acad. Sci. USA. 2013; 110:E908–E917. [PubMed: 23431170]

Chang H, Wang Y, Wu H, Nathans J. Whole mount imaging of mouse skin and its application to the analysis of hair follicle patterning and sensory axon morphology. J. Vis. Exp. 2014:e51749. [PubMed: 24999071]

Copley CO, Duncan JS, Liu C, Cheng H, Deans MR. Postnatal refinement of auditory hair cell planar polarity deficits occurs in the absence of *Vangl2*. J. Neurosci. 2013; 33:14001–14016. [PubMed: 23986237]

Curtin JA, Quint E, Tsipouri V, Arkell RM, Cattanach B, Copp AJ, Henderson DJ, Spurr N, Stanier P, Fisher EM, Nolan PM, Steel KP, Brown SD, Gray IC, Murdoch JN. Mutation of Celsr1 disrupts planar polarity of inner ear hair cells and causes severe neural tube defects in the mouse. Curr. Biol. 2003; 13:1129–1133. [PubMed: 12842012]

Dassule HR, Lewis P, Bei M, Maas R, McMahon AP. Sonic hedgehog regulates growth and morphogenesis of the tooth. Development. 2000; 127:4775–4785. [PubMed: 11044393]

Devenport D, Fuchs E. Planar polarization in embryonic epidermis orchestrates global asymmetric morphogenesis of hair follicles. Nat. Cell. Biol. 2008; 10:1257–1268. [PubMed: 18849982]

Feynman, RP.; Leighton, RB.; Sands, ML. The Feynman Lectures on Physics. Vol. 2. Reading, MA: Addison Wesley; 1963. Magnetic Materials.

Goodrich LV, Strutt D. Principles of planar polarity in animal development. Development. 2011; 128:1877–1892.

Gorski JA, Talley T, Qiu M, Puelles L, Rubenstein JL, Jones KR. Cortical excitatory neurons and glia, but not GABAergic neurons, are produced in the Emx1-expressing lineage. J. Neurosci. 2002; 22:6309–6314. [PubMed: 12151506]

Guo N, Hawkins C, Nathans J. Frizzled6 controls hair patterning in mice. Proc. Natl. Acad. Sci. S A. 2004; 101:9277–9281.

Harfe BD, Scherz PJ, Nissim S, Tian H, McMahon AP, Tabin CJ. Evidence for an expansion-based temporal Shh gradient in specifying vertebrate digit identities. Cell. 2004; 118:517–528. [PubMed: 15315763]

Hayashi S, Lewis P, Pevny L, McMahon AP. Efficient gene modulation in mouse epiblast using a Sox2Cre transgenic mouse strain. Gene Expr. Patterns. 2002; 2:93–97. [PubMed: 12617844]

Hinoi T, Akyol A, Theisen BK, Ferguson DO, Greenson JK, Williams BO, Cho KR, Fearon ER. Mouse model of colonic adenoma-carcinoma progression based on somatic Apc inactivation. Cancer Res. 2007; 67:9721–9730. [PubMed: 17942902]

Hua ZL, Chang H, Wang Y, Smallwood PM, Nathans J. Partial inter-changeability of Fz3 and *Fz6* in tissue polarity signaling for epithelial orientation and axon growth and guidance. Development. 2014a; 141:3944–3954. [PubMed: 25294940]

Hua ZL, Smallwood PM, Nathans J. Frizzled3 controls axonal development in distinct populations of cranial and spinal motor neurons. Elife. 2013; 2:e01482. [PubMed: 24347548]

Hua ZL, Jeon S, Caterina MJ, Nathans J. Frizzled3 is required for the development of multiple axon tracts in the mouse central nervous system. Proc. Natl. Acad. Sci. USA. 2014b; 111:E3005–E3014. [PubMed: 24799694]

Jenny A. Planar cell polarity signaling in the Drosophila eye. Curr. Top. Dev. Biol. 2010; 93:189–227. [PubMed: 20959167]

Jones C, Cyan D, Kim SM, Li S, Ren D, Knapp L, Sprinzak D, Avraham KB, Matsuzaki F, Chi F, Chen P. Ankrd6 is a mammalian functional homolog of Drosophila planar cell polarity gene diego and regulates coordinated cellular orientation in the mouse inner ear. Dev. Biol. 2014; 395:62–72. [PubMed: 25218921]

Kaufman, MH. The Atlas of Mouse Development. San Diego: Academic Press; 1992.

Lyuksyutova AI, Lu CC, Milanesio N, King LA, Guo N, Wang Y, Nathans J, Tessier-Lavigne M, Zou Y. Anterior-posterior guidance of commissural axons by Wnt-frizzled signaling. Science. 2003; 302:1984–1988. [PubMed: 14671310]

Mesa KR, Rompolas P, Zito G, Myung P, Sun TY, Brown S, Gonzalez DG, Blagoev KB, Haberman AM, Greco V. Niche-induced cell death and epithelial phagocytosis regulate hair follicle stem cell pool. Nature. 2015; 522:94–97. [PubMed: 25849774]

Montcouquiol M, Rachel RA, Lanford PJ, Copeland NG, Jenkins NA, Kelley MW. Identification of *Vangl2* and Scrb1 as planar polarity genes in mammals. Nature. 2003; 423:173–177. [PubMed: 12724779]

Nagy, A.; Gertsenstein, M.; Vintersten, K.; Behringer, R. Manipulating the Mouse Embryo: A Laboratory Manual. Cold Spring Harbor, New York: Cold Spring Harbor Laboratory Press; 2003.

Ohata S, Nakatani J, Herranz-Perez V, Cheng J, Belinson H, Inubushi T, Snider WD, Garcia-Verdugo JM, Wynshaw-Boris A, Alvarez-Buylla A. Loss of Dishevelleds disrupts planar polarity in ependymal motile cilia and results in hydrocephalus. Neuron. 2014; 83:558–571. [PubMed: 25043421]

Pryor SE, Massa V, Savery D, Andre P, Yang Y, Greene ND, Copp AJ. Vangl-dependent planar cell polarity signalling is not required for neural crest migration in mammals. Development. 2014; 141:3153–3158. [PubMed: 25038043]

Ravni A, Cm Y, Goffinet AM, Tissir F. Planar cell polarity cadherin Celsr1 regulates skin patterning in the mouse. J. Invest. Dermatol. 2009; 129:2507–2509. [PubMed: 19357712]

Ross, MN.; Pawlina, W. Histology: a Text and Atlas. Philadelphia: Lippincott, Williams, and Wilkins; 2011. Integumentary System; p. 488-524.

Shi D, Komatsu K, Hirao M, Toyooka Y, Koyama H, Tissir F, Goffinet AM, Uemura T, Fujimori T. Celsr1 is required for the generation of polarity at multiple levels of the mouse oviduct. Development. 2014; 141:4558–4568. [PubMed: 25406397]

Song H, Hu J, Chen W, Elliott G, Andre P, Gao B, Yang Y. Planar cell polarity breaks bilateral symmetry by controlling ciliary positioning. Nature. 2010; 466:378–382. [PubMed: 20562861]

Struhl G, Casal J, Lawrence PA. Dissecting the molecular bridges that mediate the function of Frizzled in planar cell polarity. Development. 2012; 139:3665–3674. [PubMed: 22949620]

Strutt H, Strutt D. Long-range coordination of planar polarity in Drosophila. Bioessays. 2005; 27:1218–1227. [PubMed: 16299762]

Tissir F, Bar I, Jossin Y, De Backer O, Goffinet AM. Protocadherin Celsr3 is crucial in axonal tract development. Nat. Neurosci. 2005; 8:451–457. [PubMed: 15778712]

Tissir F, Cm Y, Montcouquiol M, Zhou L, Komatsu K, Shi D, Fujimori T, Labeau J, Tyteca D, Courtoy P, Poumay Y, Uemura T, Goffinet AM. Lack of cadherins Celsr2 and Celsr3 impairs ependymal ciliogenesis, leading to fatal hydrocephalus. Nat. Neurosci. 2010; 13:700–707. [PubMed: 20473291]

Torban E, Patenaude AM, Lederc S, Rakowiecki S, Gauthier S, Andelfinger G, Epstein DJ, Gros P. Genetic interaction between members of the Vangl family causes neural tube defects in mice. Proc. Natl. Acad. Sci. USA. 2008; 105:3449–3454. [PubMed: 18296642]

Vladar EK, Bayly RD, Sangoram AM, Scott MP, Axelrod JD. Microtubules enable the planar cell polarity of airway cilia. Curr. Biol. 2012; 22:2203–2212. [PubMed: 23122850]

Wang J, Mark S, Zhang X, Ojan D, Yoo SJ, Radde-Gallwitz K, Zhang Y, Lin X, Collazo A, Wynshaw-Boris A, Chen P. Regulation of polarized extension and planar cell polarity in the cochlea by the vertebrate PCP pathway. Nat. Genet. 2005; 37:980–985. [PubMed: 16116426]

Wang Y, Badea T, Nathans J. Order from disorder: self-organization in mammalian hair patterning. Proc. Natl. Acad. Sci. USA. 2006a; 103:19800–19805. [PubMed: 17172440]

Wang Y, Chang H, Nathans J. When whorls collide: the development of hair patterns in frizzled 6 mutant mice. Development. 2010; 137:4091–4099. [PubMed: 21062866]

Wang Y, Guo N, Nathans J. The role of Frizzled3 and Frizzled6 in neural tube closure and in the planar polarity of inner-ear sensory hair cells. J. Neurosci. 2006b; 26:2147–2156. [PubMed: 16495441]

Wang Y, Thekdi N, Smallwood PM, Macke JP, Nathans J. Frizzled-3 is required for the development of major fiber tracts in the rostral CNS. J. Neurosci. 2002; 22:8563–8573. [PubMed: 12351730]

Wu H, Luo J, Yu H, Rattner A, Mo A, Wang Y, Smallwood PM, Erlanger B, Wheelan SJ, Nathans J. Cellular resolution maps of X chromosome inactivation: implications for neural development, function, and disease. Neuron. 2014; 81:103–119. [PubMed: 24411735]

Yang H, Xie X, Deng M, Chen X, Can L. Generation and characterization of Atohl-Cre knock-in mouse line. Genesis. 2010; 48:407–413. [PubMed: 20533400]

Yin H, Copley CO, Goodrich LV, Deans MR. Comparison of phenotypes between different vangl2 mutants demonstrates dominant effects of the Looptail mutation during hair cell development. PLOS One. 2012; 7:e31988. [PubMed: 22363783]

Zhou L, Bar I, Achouri Y, Campbell K, De Backer O, Hebert JM, Jones K, Kessaris N, de Rouvroit CL, O'Leary D, Richardson WD, Goffinet AM, Tissir F. Early forebrain wiring: genetic dissection using conditional Celsr3 mutant mice. Science. 2008; 320:946–949. [PubMed: 18487195]

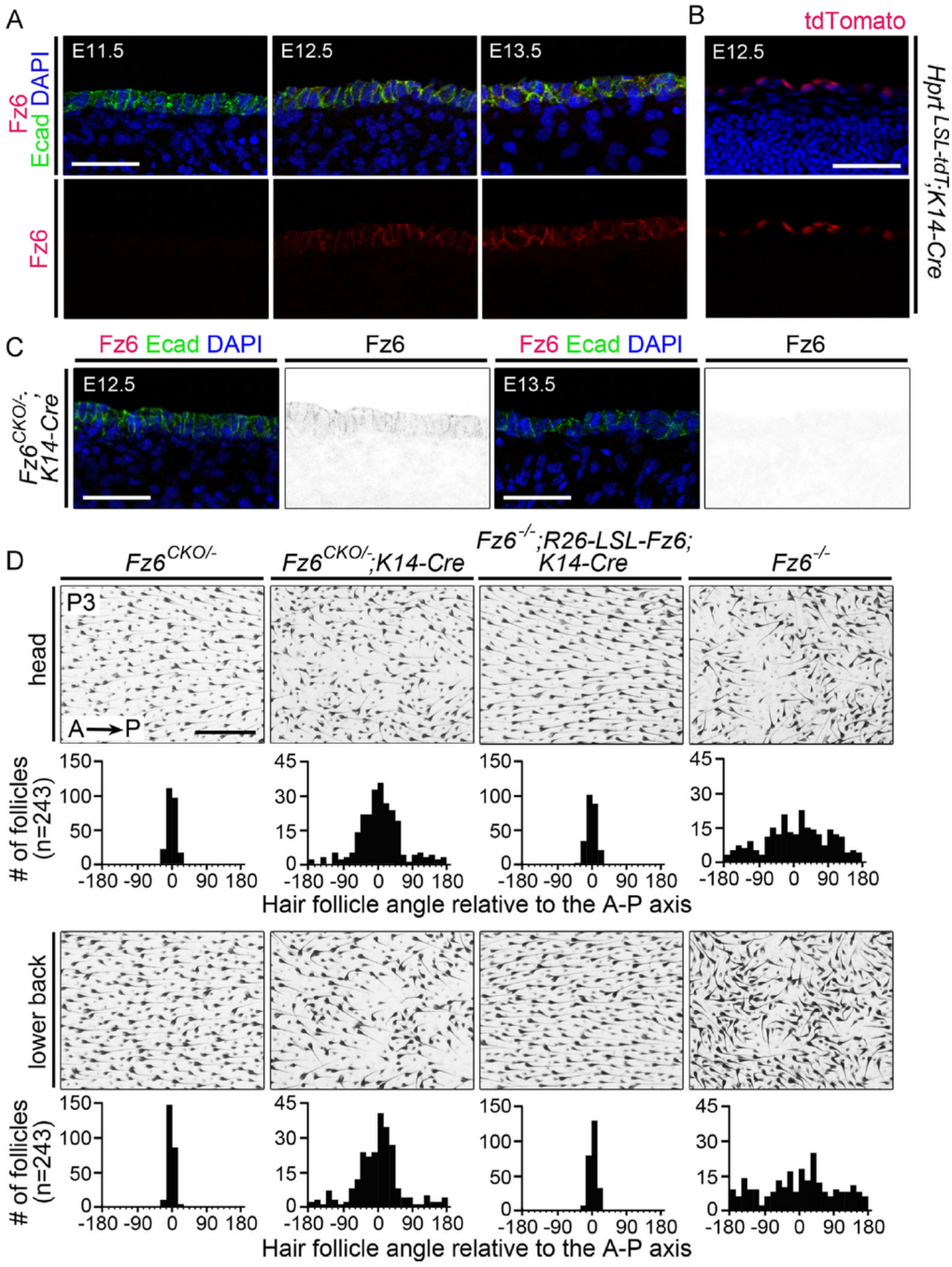

Fig. 1.

The critical time window for Fz6-dependent PCP signaling in the epidermis. (A) Immunostaining for Fz6 and E-cadherin shows that epithelial expression of *Fz6* is first detected at E12.5 in *WT* back skin. (B) *K14-Cre* recombines the *Hprt-LSL-tdT* reporter in skin epithelial cells beginning at E12.5.(C) Immunostaining for Fz6 and E-cadherin in $Fz6^{CKO/-}$;*K14-Cre* embryos shows that epithelial accumulation of Fz6 is detectable at low level at E12.5 and is undetectable at E13.5. Scale bar in A–C, 50 μm. (D) Flat mounts of head and lower back skin at P3 from $Fz6^{CKO/-}$ (phenotypically *WT*), $Fz6^{CKO/-}$;*K14-Cre,*

Fz6$^{-/-}$*;R26-LSL-Fz6;K14-Cre and Fz6*$^{-/-}$ mice. Quantifications of follicle angles relative to the anterior-posterior (A–P) axis are shown for each genotype beneath a representative flat mount image (n = 3 mice per genotype; see Materials and Methods for further details). Zero degrees corresponds to the anterior-to-posterior vector; 180 and −180 degrees correspond to the posterior-to-anterior vector. *Fz6*$^{CKO/-}$*;K14-Cre* mice show a partial hair follicle orientation phenotype, and *Fz6*$^{-/-}$*;R26-LSL-Fz6;K14-Cre* mice show normal hair follicle orientations. Scale bar, 0.5 mm.

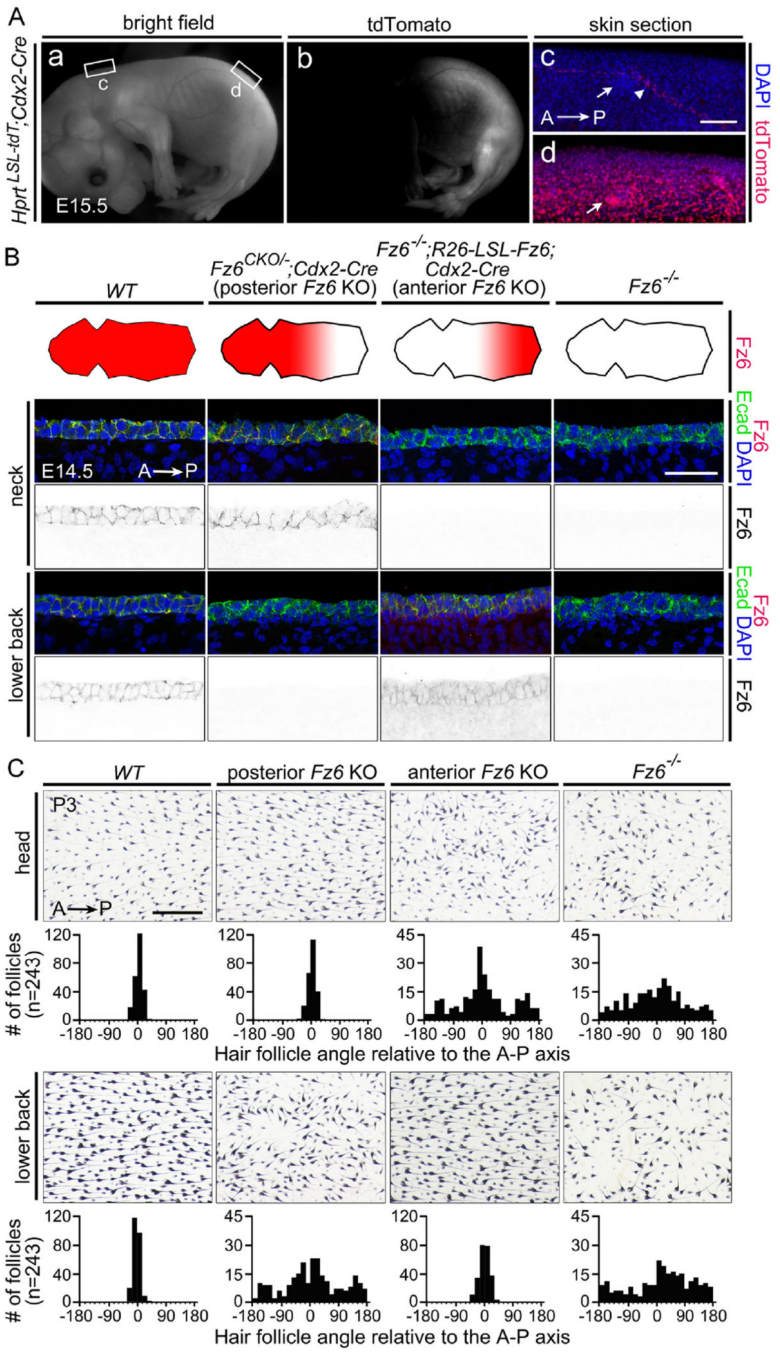

Fig. 2.

Selective deletion of *Fz6* in the anterior or posterior of the embryo leads to regional loss of follicle orientation. (A) *Cdx2-Cre* recombines the *Hprt-LSL-tdT* reporter throughout the posterior embryo, with the boundary between expressing and non-expressing tissue approximately at the level of the umbilical vessels. Inset rectangles marked (c) and (d) are enlarged to the right. Arrows in panel (c) and (d) point to hair follicles; the arrowhead in (c) points to a blood vessels, the only structures that show Cre-mediated activation of the tdTomato reporter anterior to the mid-abdominal boundary. A, anterior; P, posterior. Scale

bar, 100 μm.(B) Elimination of *Fz6* in the anterior or posterior halves of the embryo. The four schematics show a flat-mounted dorsal mouse skin with the head to the left. The territory of *Fz6* expression is indicated in red. Lower panels, immunostaining for Fz6 and E-cadherin confirms the territorial expression diagrammed above. Scale bar, 50 μm. (C) Follicle orientations in the head (upper panels) and lower back (lower panels) in P3 skin flat mounts from mice with the same four genotypes as shown in panel (B). See Methods section for details on quantification. Scale bar, 0.5 mm.

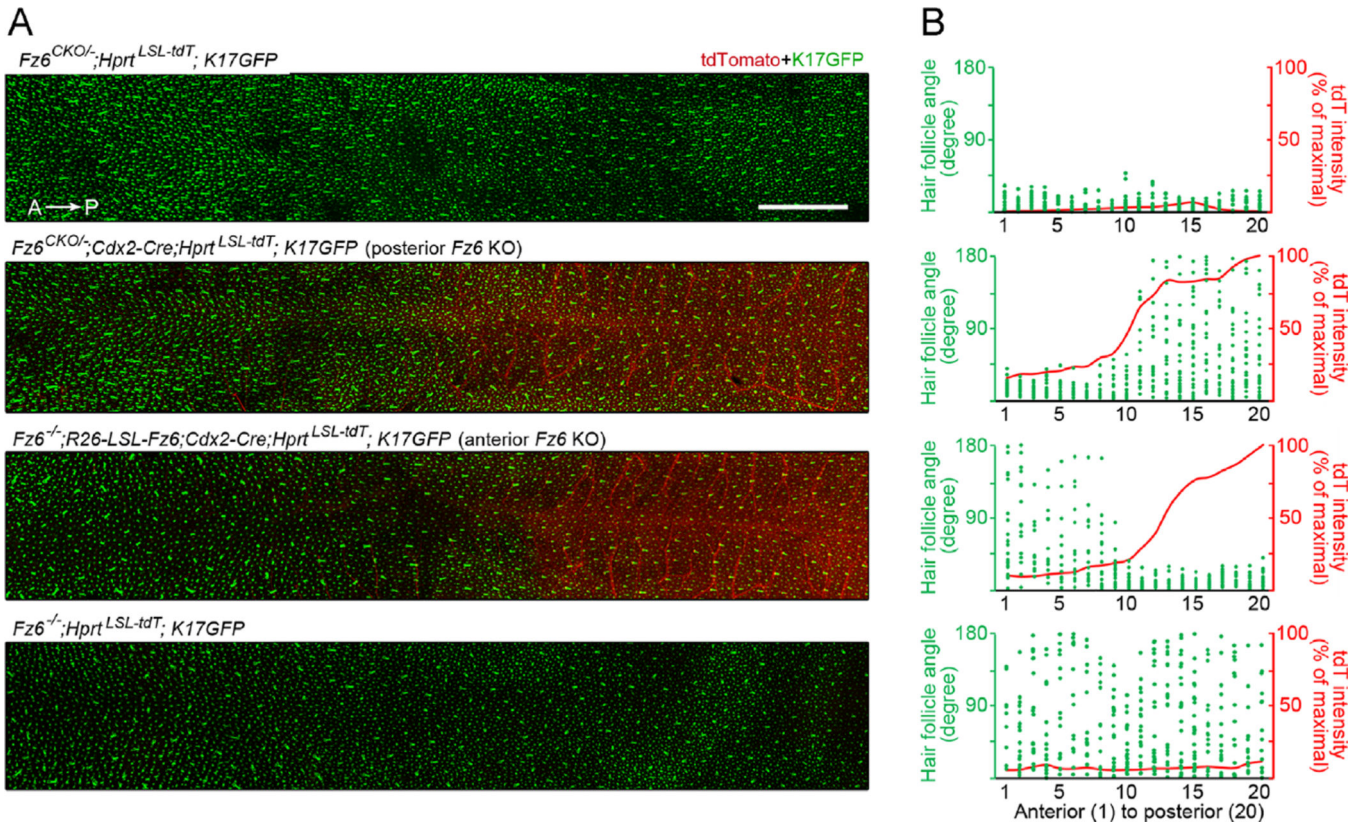

Fig. 3.

Quantification at high spatial resolution of hair follicle orientations in back skin at E17.5 in response to anterior or posterior loss of *Fz6*. (A) Montage of confocal images of back skin flat mounts. Hair follicles are visualized with a *K17-GFP* reporter and the zone of *Cdx2-Cre* activity is visualized with a *Hprt-LSL-tdT* reporter. The *Hprt-LSL-tdT* reporter was shown previously to express most strongly in vascular endothelial cells (Wu et al., 2014), a pattern confirmed here. Scale bar, 2 mm. (B) The images in (A) were divided into 20 bins of equal width along the A–P axis, and within each bin the orientations of the most mature (guard) hair follicles were determined. The plots shows angles for each guard hair follicle (green dots) and the normalized tdT intensity (red line) within each bin.

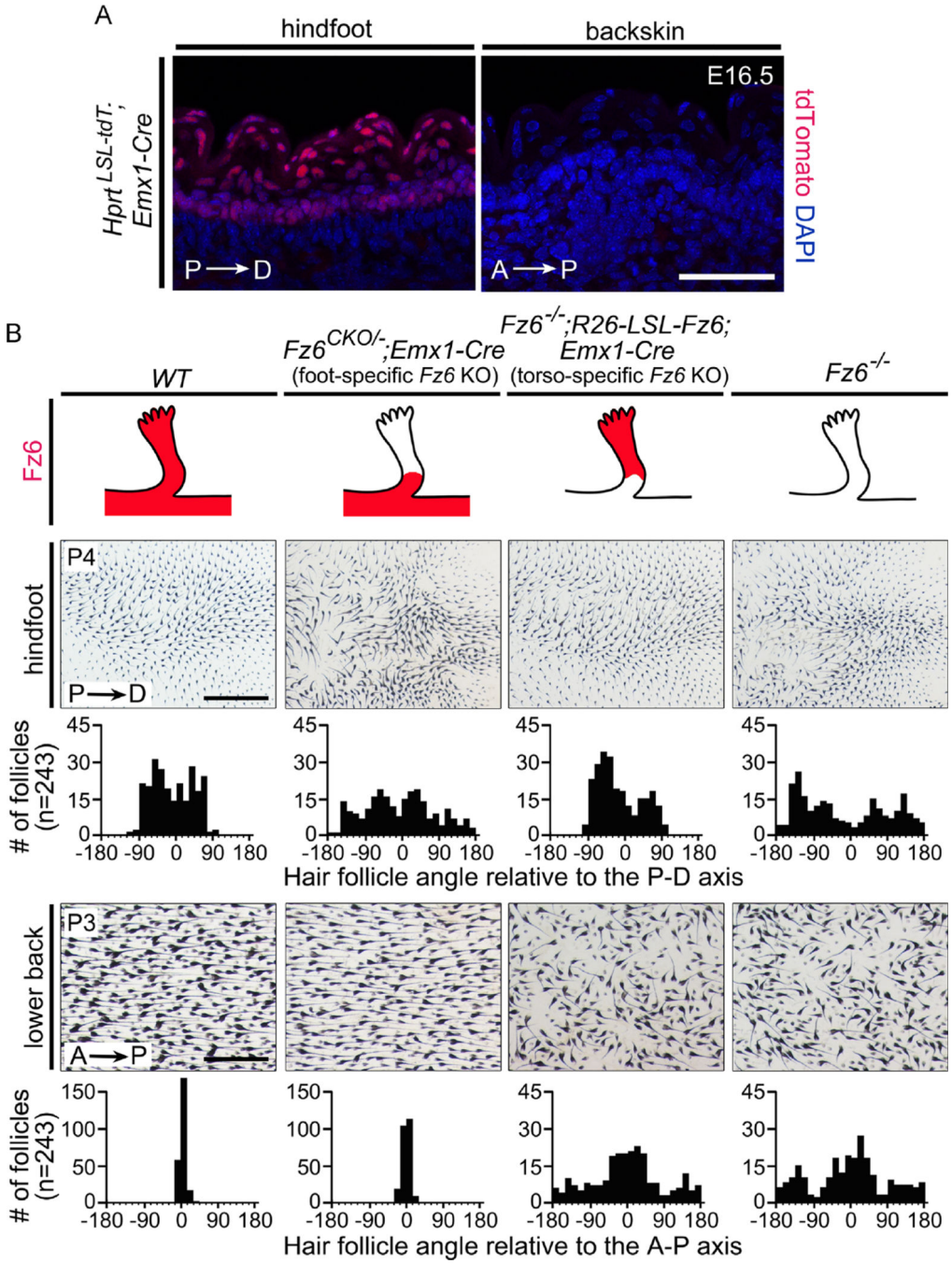

Fig. 4.

Expression or elimination of *Fz6* in the epidermis of the feet leads to regional retention or loss, respectively, of hair follicle orientation. (A) *Emx1-Cre* recombines the *Hprt-LSL-tdT* reporter in the epidermis of the hindfoot but not the back. P, proximal; D, distal. Scale bar, 50 μm. (B) Upper panels: genotypes that express or eliminate *Fz6* in the epidermis of the feet. The four schematics show a hindfoot with the territory of *Fz6* expression indicated in red. Lower panels: follicle orientations on the hindfeet at P4 and the back at P3 in skin flat

mounts. See Methods section for details on quantification. Scale bars, 1 mm (feet) and 0.5 mm (back).

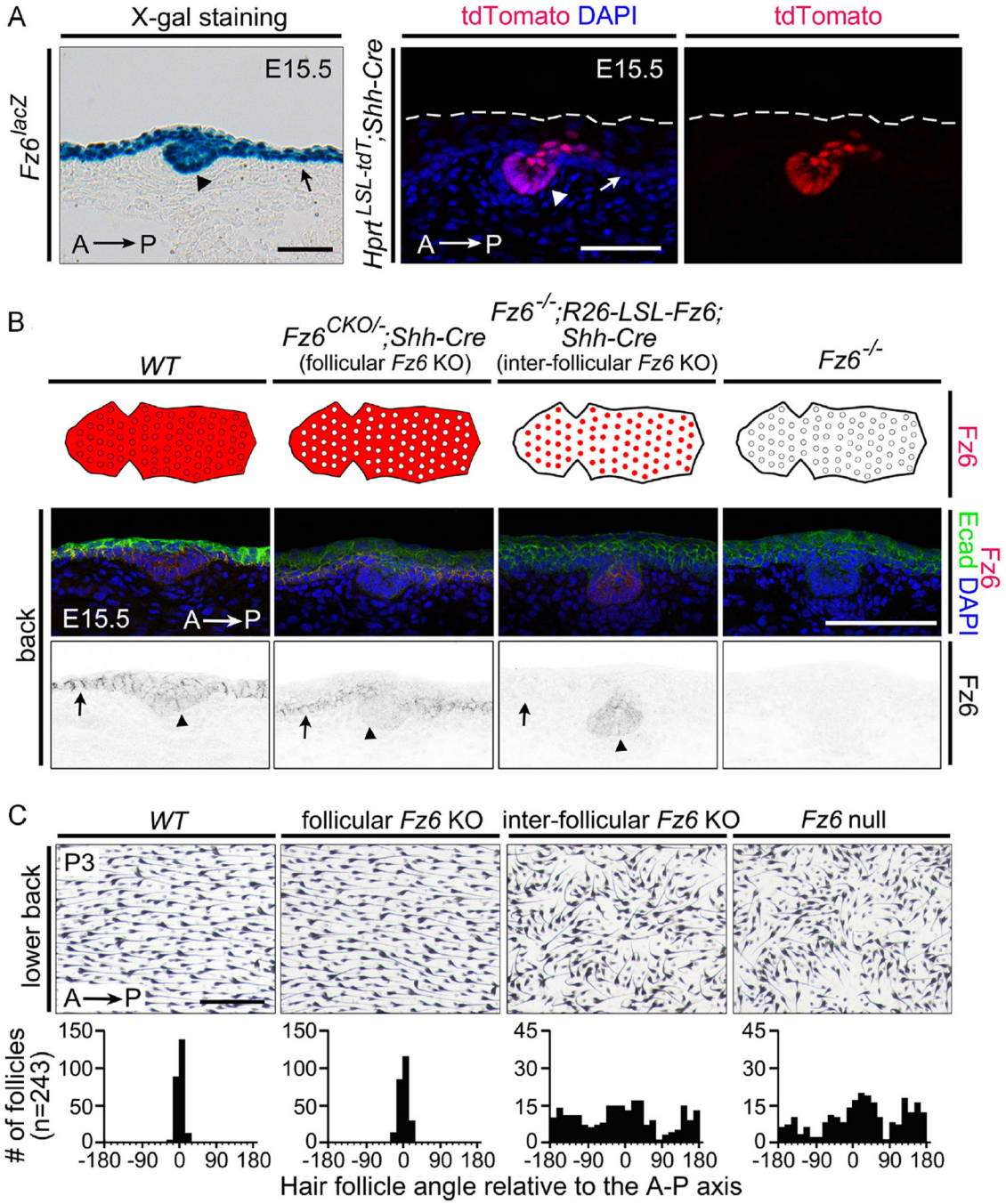

Fig. 5.

Dependence of hair follicle orientation on *Fz6* expression in the inter-follicular epidermis. (A) Left panel: expression of *Fz6* in both hair follicle cells and inter-follicular epidermis assessed by X-gal staining of a cross-section from an E15.5 $Fz6^{lacZ}$ embryo. Right panels: *Shh-Cre* recombines the *Hprt-LSL-tdT* reporter in hair follicle epithelial cells but not in the surface epidermis. The skin surface is marked by dashed lines. Scale bars, 50 μm. (B) Exclusive expression or knockout of *Fz6* in hair follicle epithelial cells by *Shh-Cre*. The schematics show a whole-mount view of back skin with hair follicles (circles) and the

surrounding surface epidermis. Anterior is to the left, and the territory of *Fz6* expression is indicated in red. Lower panels: Immunostaining for Fz6 and E-cadherin confirms the territorial expression patterns diagrammed above. Arrows, epidermis; arrowheads, hair follicles. Scale bar, 100 μm. (C) Flat mount images of back skin at P3 from mice with the same four genotypes as shown in panel (B). Beneath each image is the quantification of follicle orientations relative to the anterior-posterior (A–P) axis. Scale bar, 0.5 mm.

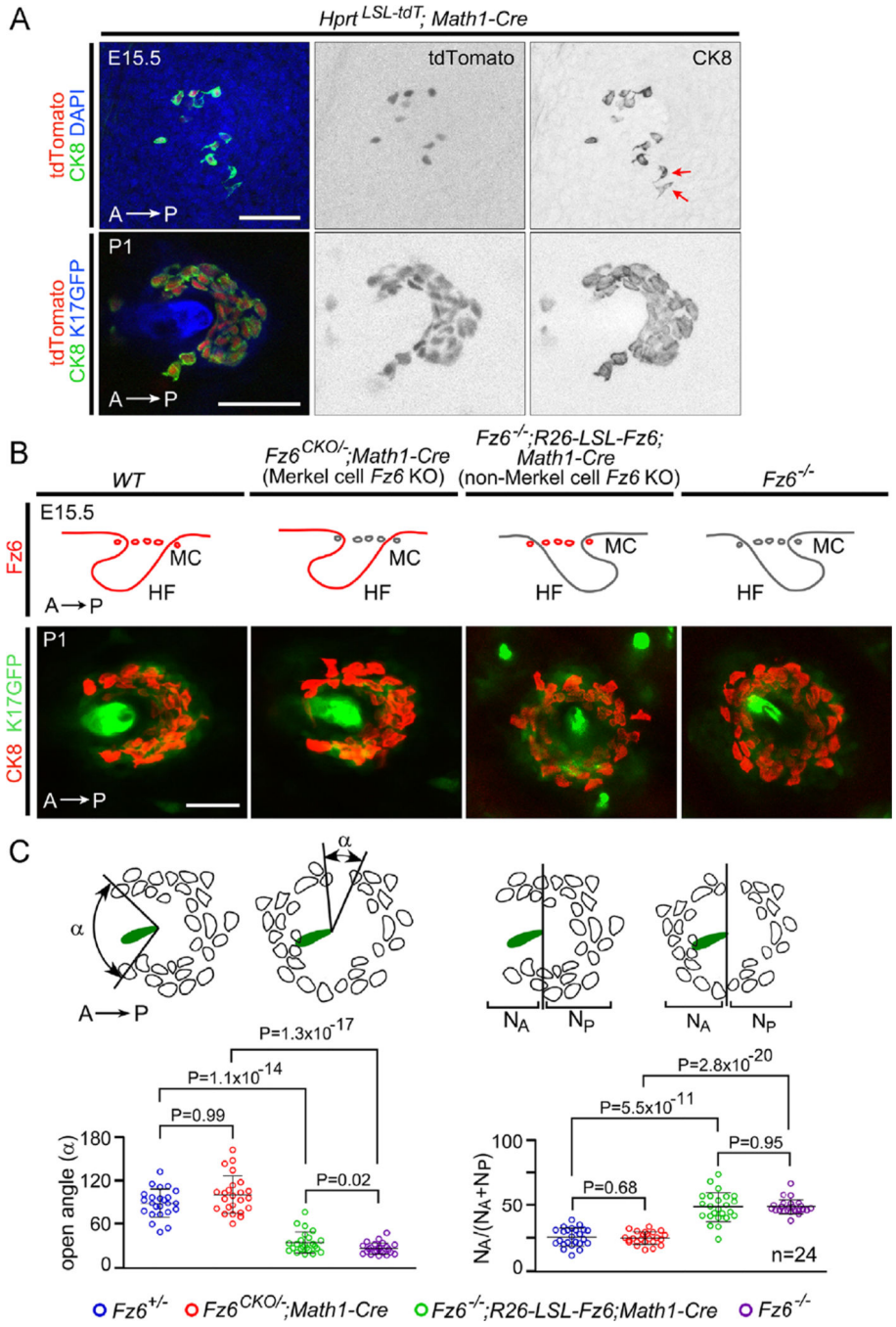

Fig. 6.

Dependence of Merkel cell cluster polarity on *Fz6* expression in the surrounding epidermis. (A) *Math1-Cre* recombines the *Hprt-LSL-tdT* reporter selectively in Merkel cells. In *Hprt-LSL-tdJ;Math1-Cre* fetuses at E15.5, Merkel cells begin to differentiate [determined by immunostaining for cytokeratin 8 (CK8)] and to express *Math1-Cre* as determined by tdTomato accumulation The presence of two CK8+ tdTomato- Merkel cells (red arrows) may reflect the time required for reporter accumulation after Cre-mediated recombination In *Hprt-LSL-tdT;Math1-Cre* at P1, tdTomato is expressed by all Merkel cells (marked by

CK8), which are arranged in a semicircle around a central guard hair follicle (marked by *K17-GFP* expression). Scale bar, 50 um (B) Top, genotypes for exclusive expression or knock out of *Fz6* in Merkel cells. The four sets of schematics show a transverse section of an E15.5 hair follicle (HF) with its associated Merkel cells (MC). Hair follicles are shown either correctly oriented (i.e. with an anterior to posterior polarity as they approach the skin surface; first and second panels) or inappropriately oriented (third and fourth panels). Anterior is to the left, and the territory of *Fz6* expression is indicated in red. Bottom, examples of flat mount images of a P1 hair follicle (marked by *K17-GFP* expression) with its associated Merkel cells (marked by CK8). Scale bar, 50 μm. (C) Diagrams showing the measurement of the open angles of Merkel cell clusters and the distributions of Merkel cells around guard follicles in flat mount skin at P1. Left, for each Merkel cell cluster, the opening angle was measured by connecting the two most distantly separated Merkel cells to the center of the hair shaft within the same Z-plane. Right, number of Merkel cells anterior (N_A) or posterior (N_P) to a line bisecting the follicle at right angles to the A–P axis. Scatterplots show results for individual Merkel cell clusters together with mean +/− SD. *P*-values, student *t*-test.

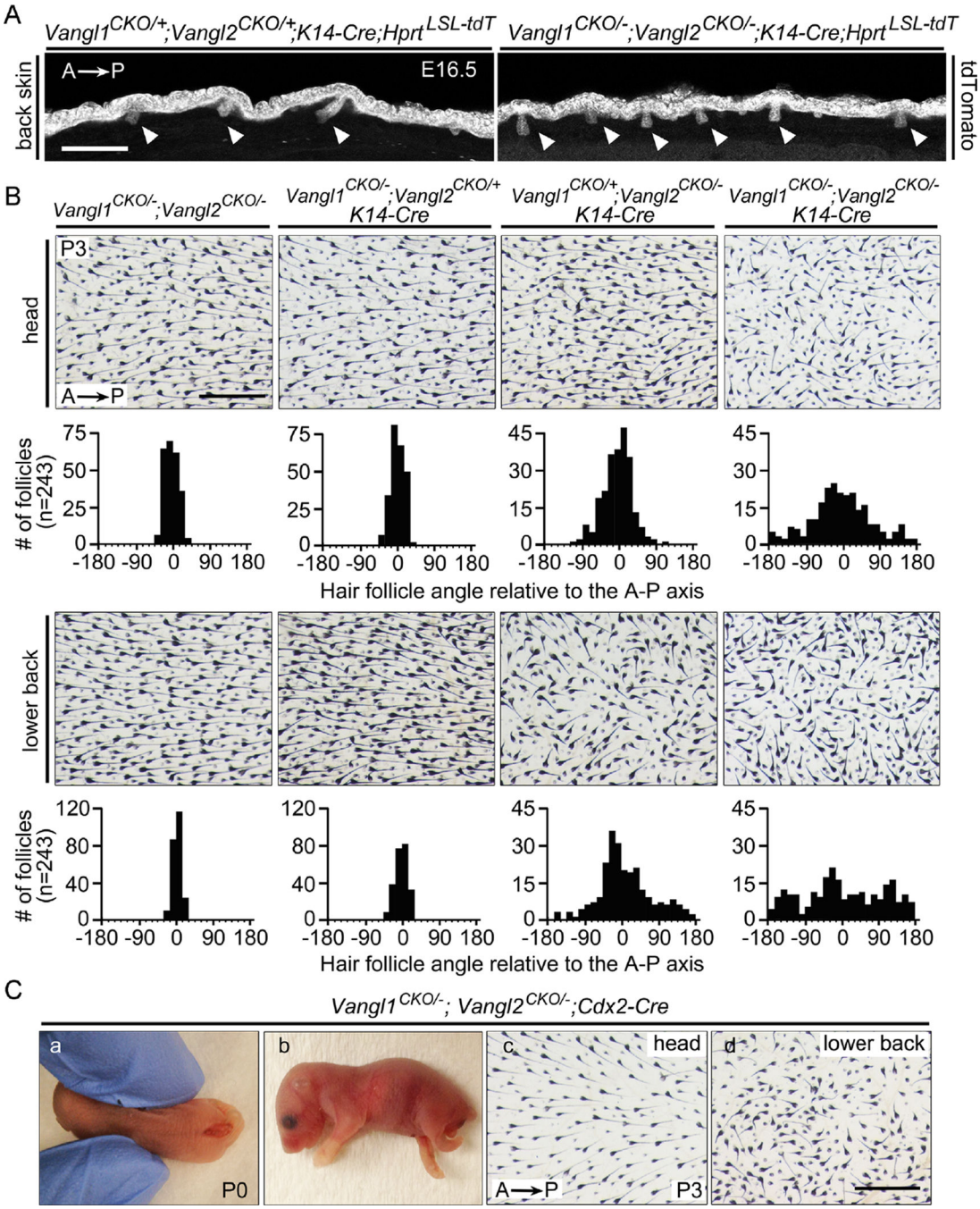

Fig. 7.

Relative importance of *Vangl1* vs. *Vangl2* in hair follicle orientation. (A) Surface epithelial cells and developing hair follicles (arrowheads) in back skin visualized with the *Hprt-LSL-tdT* reporter at E16.5. In the absence of epithelial *Vangl1* and *Vangl2*, developing follicles are oriented perpendicular to the plane of the epidermis. Scale bar, 200 μm. (B) Hair follicle orientation in head and back skin at P3 following epidermis-specific loss of two, three, or four alleles of *Vangl1* and *Vangl2*, beginning at E11.5-E12.5. Scale bar, 0.5 mm. (C) Phenotypes caused by posterior deletion of *Vangl1* and *Vangl2*. Panels (a) and (b) show

neural tube closure and hindlimb defects at P0 observed in ~95% of *Vangl1*$^{CKO/-}$;*Vangl2*$^{CKO/-}$;*Cdx2-Cre*. Panels (c) and (d) show a skin flat mount from a rare *Vangl1*$^{CKO/-}$;*Vangl2*$^{CKO/-}$;*Cdx2-Cre* mouse at P3 with a closed neural tube. Hair follicle orientations are normal on the head and aberrant on the lower back. Scale bar, 0.5 mm.

Table 1

Location and timing of *Cre* expression determined with the *Hprt-LSL-tdT* reporter.

Cre line	Location	Embryonic day
K14-Cre	epidermis on the back	E11.5 (−), E12.5 (+)
Cdx2-Cre	posterior, including the epidermis	E11.5 (+)
Emx1-Cre	limb bud ectoderm	E11.5 (+)
Shh-Cre	hair follicles	E14.5 (−), E15.5 (+)
Math1-Cre	Merkel cells	E14.5 (−), E15.5 (+)

tdTomato fluorescence was assessed by visual inspection and scored as absent/undetectable (−) or present (+).